Enhanced Crystallization of Bisphenol A Polycarbonate in Thin and Ultrathin Films by Supercritical Carbon Dioxide

ARTICLE *in* MACROMOLECULES · JULY 2011

Impact Factor: 5.8 · DOI: 10.1021/ma102797r

4 AUTHORS:

Qiaofeng Lan
Chinese Academy of Sciences
3 PUBLICATIONS **22** CITATIONS
SEE PROFILE

Jian Yu
Chinese Academy of Sciences
54 PUBLICATIONS **731** CITATIONS
SEE PROFILE

Jun Zhang
Anhui University
897 PUBLICATIONS **13,879** CITATIONS
SEE PROFILE

Jiasong He
Chinese Academy of Sciences
141 PUBLICATIONS **3,905** CITATIONS
SEE PROFILE

Macromolecules

ARTICLE

pubs.acs.org/Macromolecules

Enhanced Crystallization of Bisphenol A Polycarbonate in Thin and Ultrathin Films by Supercritical Carbon Dioxide

Qiaofeng Lan,[†,‡] Jian Yu,[*,†] Jun Zhang,[*,†] and Jiasong He[†]

[†]Beijing National Laboratory for Molecular Sciences (BNLMS), Key Laboratory of Engineering Plastics, Joint Laboratory of Polymer Science and Materials, Institute of Chemistry, Chinese Academy of Sciences, Beijing 100190, P. R. China

[‡]Graduate University of Chinese Academy of Sciences, Beijing 100039, P. R. China

ABSTRACT: The crystallization behavior of thin bisphenol A polycarbonate (PC) films after treatment in supercritical CO_2 ($ScCO_2$) was investigated by using polarized optical microscopy (POM) and atomic force microscopy (AFM). Experimental results indicated that the crystallization ability in thin PC film of 259 nm thick was higher than that in the bulk in a much wider temperature range, and the crystallization window was further broadened when the thickness of samples decreased. The 15 nm film crystallized under 20 MPa CO_2 at 60 °C, i.e., more than 90 K below the glass transition temperature of the bulk at ambient pressure, while the 259 nm film remained amorphous under the same treatment condition. The results further revealed that crystalline morphology was affected by the CO_2 treatment condition and film thickness. And the 7 nm film dewetted the substrate in the treatment at 20 MPa/60 °C instead of crystallization. It was indicated that chain mobility of the polymer was strongly increased in $ScCO_2$ when the film thickness was decreased to the scale of radius of gyration (ca. 6 nm) of the polymer. A modified three-layer model was proposed to explain these findings by introducing the effect of CO_2 adsorption. The excess CO_2 adsorbed at the free surface and polymer/substrate interface enlarged portions of these two layers and enhanced the polymer mobility therein, which took effect in thin films with thickness from hundreds down to several nanometers.

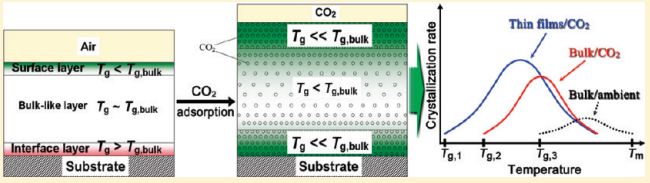

INTRODUCTION

In recent years, polymer thin films have received considerable interest due to their important technological applications such as microelectronics, coatings, and adhesion.[1−3] The structure and properties of polymers confined in thin films often deviate significantly from those of corresponding bulk polymers, especially in ultrathin films.[3−7] The glass transition temperature (T_g) and crystallization behavior of polymer thin films usually show a strong thickness dependence. Many studies have shown that the mobility of polymer chains near the surface (polymer/air interface) is higher than that in bulk.[6−11] Therefore, for freestanding films, T_g is typically decreased with decreasing film thickness when thickness is in the range of tens of nanometers.[6,7,12] On the other hand, for the substrate-supported thin films, T_g have been observed to either increase or decrease with decreasing film thickness when polymer films are sufficiently thin, depending on the specific interaction between the polymer and the substrate. Generally, a reduction in thickness leads to an increase in T_g for polymer films exhibiting strong attractive interactions with the substrate,[5,13−16] and to a reduction in T_g for ones lacking such interactions.[4−6,15−22] Studies of crystallization behavior in nanoconfined polymers have mainly focused on lamellar orientation, surface morphology, and crystal growth rate.[3,11,23−27] Moreover, the physical properties of polymer thin films are also affected to a large extent by the ambient atmosphere. For example, polymer thin films would exhibit thickness dependent properties of anomalous swelling[28−30] and retrograde vitrification[31,32] in the presence of supercritical CO_2.

Supercritical CO_2 ($ScCO_2$, $T_c = 31.1$ °C, $P_c = 7.38$ MPa) has been widely utilized as a solvent in fundamental research fields to understand the crystallization behavior of semicrystalline polymers.[33−37] The solvent properties of CO_2 can be easily modulated by simply changing the pressure and temperature, and after treatment CO_2 can be removed from polymers quickly and completely by simple depressurization process. Moreover, the plasticization effect of CO_2 usually lower the T_g[38,39] and the melting point (T_m)[39] of polymers. As a result, CO_2 accelerates the crystallization of polymers having low crystallization rate, such as bisphenol A polycarbonate (PC), and make its crystallization take place at much lower temperatures.[36,37,40]

The crystallization behaviors of PC have been extensively investigated due to its considerable scientific and technical importance.[41−45] However, it is well-known that the crystallization of pure bulk PC exhibits extremely slow crystallization kinetics, with a crystallization half-time of 12 days by only thermal treatment at 190 °C.[44] The reason for this slow kinetics is the high work of chain folding for PC (27.3 vs 5.7 kcal/mol for polyethylene) due to its chain rigidity. Therefore, some nucleating agent or plasticizers have been added to facilitate the crystallization.[41,44] In addition, organic solvents or vapors are also used to induce the crystallization of PC.[43,45] Solvents usually

Received: December 9, 2010
Revised: March 31, 2011
Published: June 22, 2011

induce the crystallization of PC rapidly, while they are very difficult to remove completely after the crystallization.

With the help of $ScCO_2$ technique, some particular behaviors of the bulk polymers having slow rate for thermal-induced crystallization have been investigated in our previous papers, including the influence of the long-chain branching on the crystallization behavior of bulk PC in $ScCO_2$.[40,46,47] Because of the confined effect thin PC films would display unique crystallization behavior in the presence of $ScCO_2$, which lacks study so far. It is expected that for PC the $ScCO_2$ treatment can avoid the difficulty in solvent-induced crystallization and the tedium in thermal treatment. In the present work, thin PC films with different thickness were prepared and treated in $ScCO_2$ to induce the crystallization. The influence of parameters such as treatment temperature, CO_2 pressure and film thickness on the crystallization behavior is discussed, based on the crystal morphology characterized by polarized optical microscopy (POM) and atomic force microscopy (AFM). A modified three-layer model describing the enhanced mobility with decreasing thickness in thin films by $ScCO_2$ is also discussed.

EXPERIMENTAL SECTION

Materials. The bisphenol A polycarbonate (PC, M_w = 35 500, M_w/M_n = 3.03) with linear chain structure was supplied as granules by Idemitsu Petrochemical Co (A2700). The T_g was 154 °C. Its radius of gyration (R_g) was ca. 6 nm by calculation. CO_2 with a purity of 99.95% was supplied by Beijing Analytical Gas Factory, China. Cyclohexanone was reagent grade and used as received.

Sample Preparation. Glass covers and silicon wafers were used as the substrate for POM and AFM observation, respectively. They were cleaned in a mixture of H_2SO_4 and H_2O_2 (70/30 vol %) for 30 min at 110 °C. After cooling to room temperature, they were thoroughly washed with deionized water and then dried under a nitrogen flow. Thin PC films with different thicknesses on both kinds of substrates were prepared by spin-coating 0.25 to 5 wt % polymer-cyclohexanone solutions at 2000 rpm speed for 60 s. After vacuum drying at room temperature for 6 h, all the thin film samples were annealed at 150 °C (close to the sample's bulk T_g) for 12 h under vacuum in order to remove residual solvent and to make sure that all samples possess a similar and well-defined thermal history before the CO_2 treatment. AFM observation confirmed that all these thermally annealed films were amorphous, which were used for the further CO_2 treatment.

$ScCO_2$ Treatment. The thin PC films were loaded in a high-pressure vessel preheated to the experimental temperature. The vessel was then flushed with low-pressure CO_2 for about 3 min and pressurized to a desired value. Once the CO_2 pressure reached the desired value, the timing began. After 6 h treatment (unless indicated), the vessel was quenched to room temperature and depressurized slowly at a rate of ca. 0.5 MPa/min.

Measurements. The thickness of amorphous PC films was measured on a J. A. Woollam M-2000 V spectroscopic ellipsometer. The spherulite morphology was observed on an Olympus BX51 POM and recorded with a connected digital camera. Tapping mode AFM images were obtained at room temperature using a NanoScope III Multi-Mode atomic force microscope (Digital Instruments). Silicon tips with a resonance frequency of 300 kHz and a spring constant of 40 $N \cdot m^{-1}$ were used. The scan rate ranged from 0.3 to 1 Hz with the scanning density of 512 lines/frame.

RESULTS AND DISCUSSION

Enhanced Crystallization Behavior of Thin PC Films in $ScCO_2$. It is suggested that the plasticization effect of $ScCO_2$ significantly increases the segmental mobility of PC chains by increasing polymer free volume,[46,48] greatly shortens the induction period of PC crystallization. In this section, the effect of CO_2 treatment temperature and pressure on the crystallization behavior of PC films of 259 nm thick was investigated on the basis of spherulite morphology characterized by optical microscopy.

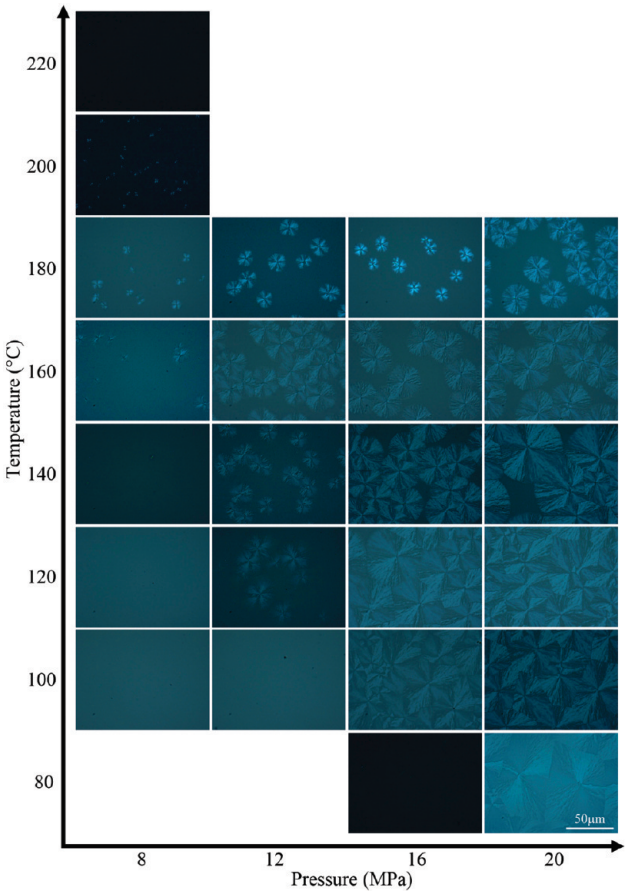

Figure 1. POM micrographs of PC films of 259 nm thick treated in CO_2 of temperature and pressure indicated for 6 h.

Figure 1 shows POM micrographs of PC films treated in $ScCO_2$ at 8−20 MPa and different temperatures in the range of 80−220 °C for 6 h. At 8 MPa, no crystal is found in films treated at 140 °C and below. When the temperature is increased to 160, 180, and 200 °C, some small spherulites with low crystal density are formed by the treatment. When the temperature is further increased to 220 °C, again no crystal is formed. This is reasonable because the nucleation ability would decrease significantly at a temperature close to the T_m. These results indicate that the PC has low crystallization ability in 8 MPa CO_2.

The images in the second column of Figure 1 show the POM results of PC films annealed in CO_2 at 12 MPa and 100−180 °C. It is shown that all the samples crystallized except the one treated at 100 °C. Furthermore, the film treated at 160 °C has the biggest crystal density and the highest crystallization degree. Therefore, the plasticization effect is enhanced by increasing the CO_2 pressure from 8 to 12 MPa.

The results of thin films treated at 16 and 20 MPa are shown in the third and fourth columns of Figure 1, respectively. It is clear that their crystallization rates are apparently enhanced. Under CO_2 at 16 MPa and low temperatures of 100 and 120 °C, PC

dx.doi.org/10.1021/ma102797r |Macromolecules 2011, 44, 5743–5749

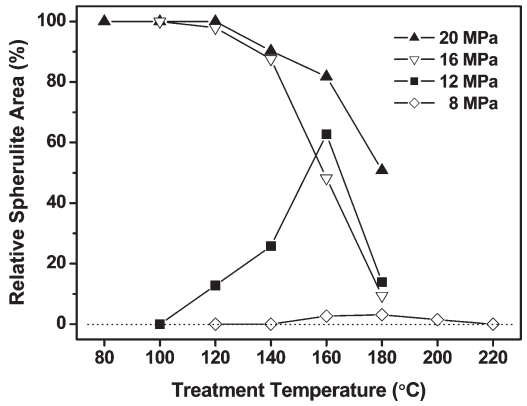

Figure 2. Area portions occupied by spherulites in the POM micrograph (data taken from Figure 1) as a function of the treatment temperature under various CO_2 pressures.

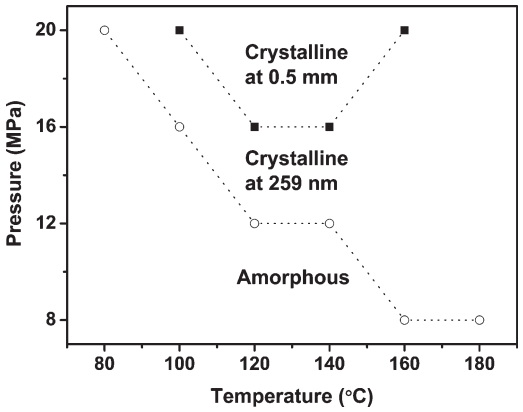

Figure 3. Crystallization window of thin PC films and bulk PC samples treated under $ScCO_2$. The treatment time for thin film (259 nm) and bulk (0.5 mm) samples was 6 and 12 h, respectively.

films crystallize completely to form impinged spherulites occupying the whole micrographs. Meanwhile, the unfilled volume in the treated films increases with the increase of temperature above 120 °C, indicating the spherulites are still in the course of crystallization due to the their slow kinetics. Under CO_2 at 20 MPa, the spherulites obtained have larger size than those obtained at 16 MPa, although their morphological difference is small. However, the impinging spherulites are formed even at temperature as low as 80 °C, which is more than 70 K lower than the PC's bulk T_g at ambient pressure. These results shown in Figure 1 clearly indicate that the plasticization effect is greatly increased to enhance the segmental mobility with the increase of CO_2 pressure.

The area ratio occupied by spherulites in the POM micrograph, representing roughly the crystallization degree and then the crystallization rate, was calculated and plotted against the treatment temperature. As shown in Figure 2, the relative crystallinity (or crystallization rate) presents a maximum value at 180 °C for those samples treated at 8 MPa. However, its value is extremely low and less than 5%. The maximum crystallinity increases sharply between the pressure of 8 and 16 MPa, after that it remains approximately constant up to 20 MPa. On the other hand, the temperature corresponding to the maximum crystallinity (T_{max}) decreases with the increase of treatment pressure, i.e., from 180 °C at 8 MPa to 160 °C at 12 MPa, then to 100 °C at 16 MPa. For higher treatment pressure of 20 MPa, it is difficult to distinguish the T_{max} due to the micrographs totally occupied by spherulites when the temperature is in the range of 80−120 °C. Consequently, the shape of those curves shown in Figure 2 is consistent with that of the bell-shaped dependence of the crystallization rate on the crystallization temperature in general. The latter also has a maximum between T_g and T_m originating from the nucleation controlled mechanism at low undercooling and crystal growth controlled one at high undercooling. Therefore, the T_{max} for thin PC films is expected to shift to lower temperature in the presence of $ScCO_2$, because both T_g and T_m of polymer bulk are depressed in comparison to those displayed at ambient pressure,[38−40] and the T_{max} decreases with the increase of CO_2 pressure, resulted from the enhanced polymer mobility due to plasticization effect.

Accordingly, the general crystallization window in $ScCO_2$ is obtained in Figure 3 for thin PC films of 259 nm thick. The results of bulk PC samples (0.5 mm thick) are also presented for comparison.[40] The treatment time was 6 and 12 h for PC films and bulk samples, respectively. Two dotted curves shown in Figure 3 represent the boundary of the temperature range of crystallization. Samples treated under the conditions below the curves are amorphous, while above are crystallized. At 8 MPa, the PC film is only induced to crystallize at 160 and 180 °C. Then the temperature range is broadened with the increase of the treatment pressure, i.e., 120−180 °C at 12 MPa, and 100−180 °C at 16 MPa. At the highest pressure of 20 MPa used in this study, the lowest crystallization temperature for thin films is further decreased to 80 °C. By comparison, the bulk samples show a higher pressure threshold of 16 MPa for crystallization, and a narrower crystallization temperature range of 100−160 °C even under 20 MPa $ScCO_2$. These results indicate that PC was induced to crystallize in a broadened range of temperature and pressure, when the sample changed from bulk (0.5 mm) to thin film (259 nm).

Crystal Morphology of Thin PC Films after Treatment in $ScCO_2$. In order to observe fine morphological details of thin PC films, especially for those with thickness close to R_g, AFM characterization was further performed on PC films treated by $ScCO_2$. In this section, the crystallization behaviors of thin and ultrathin films are discussed based on the influences of treatment temperature, CO_2 pressure, and film thickness on the morphology and structure.

Influence of Treatment Temperature. Figure 4 shows AFM topographic images of $ScCO_2$-induced crystalline morphology of the thin films of 259 nm and ultrathin films of 15 nm, respectively. The treatment was conducted under CO_2 at 20 MPa and 100, 120, 140, and 160 °C. As shown in parts a−d of Figure 4, the regular spherulites with typical morphology are formed and impinged to each other, which are consistent with the POM results. The compact crystals having well-defined boundaries contain a center, from which the crystalline lamellae splay out to fill up the volume of the film. The size of crystalline fibrils seems to decrease with the increase of treatment temperature, and the needlelike morphology of spherulite branches become increasingly fine. When the thickness is decreased from 259 to 15 nm, which is about 2.5 R_g, the morphologies of PC films after treatment are totally different, as shown in Figure 4, parts e−h. At the low temperature of 100 °C, the spherulitic structure becomes more open. With the increase of the temperature, the spherulites split, and the crystalline structure becomes more and

dx.doi.org/10.1021/ma102797r |*Macromolecules* 2011, 44, 5743–5749

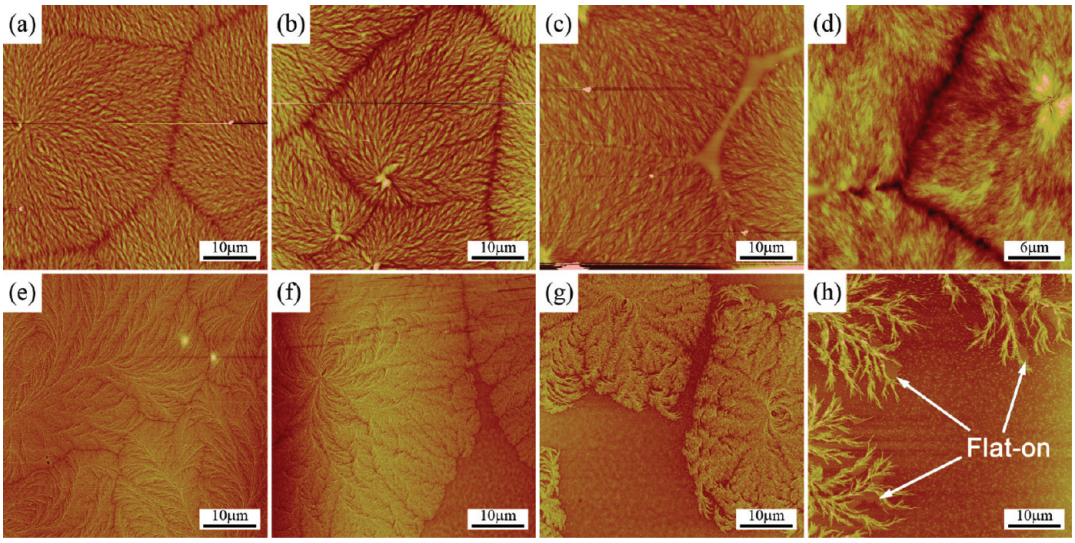

Figure 4. AFM height images of PC films of 259 nm thick (upper row) and 15 nm thick (lower row) treated in CO_2 of 20 MPa and different temperatures for 6 h: (a, e) 100, (b, f) 120, (c, g) 140, and (d, h) 160 °C.

more diffusive. Seaweed structure appears in the sample treated at 140 °C, while isolated dendritic morphology is formed at 160 °C. Additionally, flat-on lamellae are formed in PC film of 15 nm at 160 °C, as pointed by the arrows in Figure 4h. The change in morphology with undercooling is similar to other reported experimental results and theoretical simulations.[27,49−51] At high temperature (low undercooling), where the driving force is not large enough to initiate homogeneous nucleation, the heterogeneous nucleation at surface/interface of films become important, resulting in branched structures, especially for those films with smaller thicknesses. These results indicate that the crystalline morphology shows a strong dependence on the treatment temperature, especially for the films having thickness close to several R_g.

Influence of CO_2 Pressure. As mentioned above, after the treatment in $ScCO_2$ at 160 °C, the morphology of PC films with different thicknesses had the highly significant difference, i.e., from dense branching spherulitic structure for 259 nm film (Figure 4d), to dendritic structure for 15 nm one (Figure 4h). Therefore, the treatment temperature of 160 °C was used in the following experiments to study the influence of pressure and film thickness on the crystalline morphology of PC films.

Figure 5 shows AFM height images of PC films with thicknesses of 259 and 45 nm after the treatment in $ScCO_2$ at 160 °C and different pressures. After the treatment at 20 MPa, both PC films are induced to crystallize completely to develop split and diffusive branches, mostly because of the strong plasticization effect even though they have distinct morphologies. When the treatment pressure is decreased to 8 MPa, the 259 nm film only develops few incomplete spherulites at their initial course of growth (Figure 5c), indicating a low crystal growth rate due to the low mobility of PC chains under low CO_2 pressure. These results are consistent with the morphology and crystallinity revealed by POM (Figure 1). In contrast, the 45 nm film displays well-developed impinged spherulites with coarse branches composed of fibril bundles (Figure 5d), in comparison with those formed at 20 MPa shown in Figure 5b.

Influence of Film Thickness. From the results of 20 MPa, it is observed that the crystal branching became more and more loose

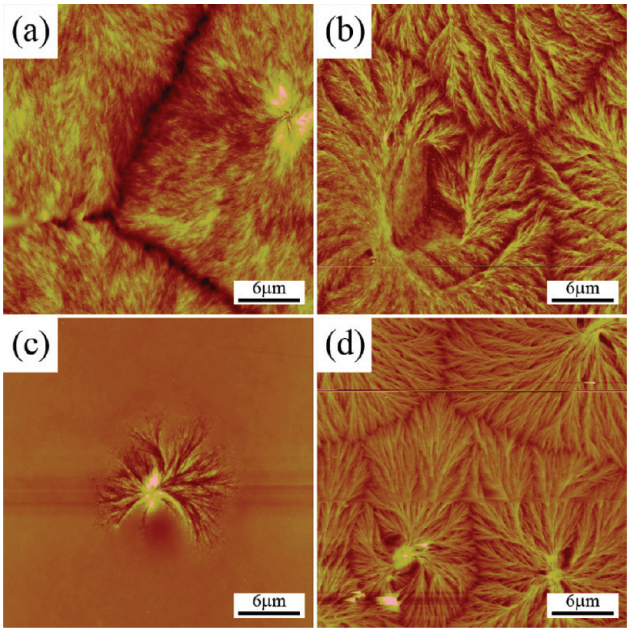

Figure 5. AFM height images of PC films with different thicknesses treated in CO_2 of different pressures at 160 °C for 6 h. Key: (a) 259 nm, 20 MPa; (b) 45 nm, 20 MPa; (c) 259 nm, 8 MPa; (d) 45 nm, 8 MPa.

when the film thickness decreases from 259 to 45 nm, however they are still compact as shown in Figure 5, parts a and b, respectively. When the thickness further decreases to 15 nm, the branches are apart from each other to form isolated dendritic morphology, as mentioned above (Figure 4h). Under CO_2 of 8 MPa, the film with thinner thickness of 45 nm crystallizes completely, while the thicker film of 259 nm forms merely incomplete crystals, indicating a very low crystallization rate. Therefore, the effect of film thickness is more significant when the CO_2 pressure decreases to a lower value.

Results shown above indicate that the film thickness indeed plays an important role in the crystallization of polymer thin films

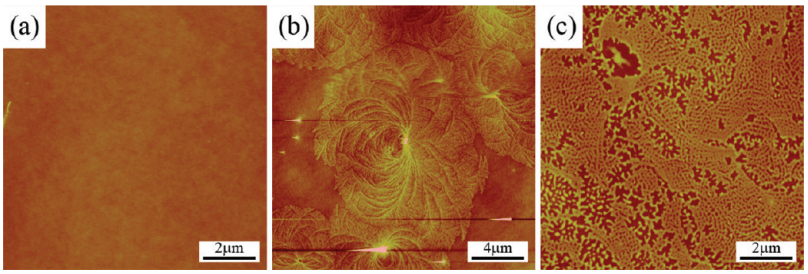

Figure 6. AFM height images of PC films with different thicknesses treated in CO_2 of 20 MPa and 60 °C for 12 h: (a) 259 nm, (b) 15 nm, and (c) 7 nm.

under CO_2. The dynamics of polymer chains is greatly increased in the presence of CO_2 for the ultrathin films, while they are topologically constrained under ambient pressure. The effect of film thickness on the polymer chain mobility is further revealed at much low temperature of 60 °C under CO_2. As shown in Figure 6, a dense branching spherulitic structure is observed in the 15 nm film treated at 20 MPa and 60 °C for 12 h. However, for the 259 nm film, there is no crystal after the treatment under the same condition (Figure 6a). Bulk PC sample also can not crystallize after treatment under CO_2 at 20 MPa and 60 °C, although the equilibrium CO_2 adsorption amount is about 11 wt %.[52] Therefore, when the thickness is reduced to 15 nm, the temperature for inducing crystallization at 20 MPa shifts to a value more than 90 K below the normal T_g at ambient pressure. This temperature is outside the crystallization window for the 259 nm film shown in Figure 3.

On the other hand, when the thickness further decreases to 7 nm, lots of randomly distributed holes are produced after treatment at 20 MPa and 60 °C for 12 h (Figure 6c). It indicates that a dewetting process occurred in the film with the thickness close to the R_g of PC chain, instead of crystallization. It is well-known that dewetting is a phenomenon resulted from the breakup of thin film into droplets eventually on substrate surfaces due to the high mobility of polymer.[53,54]

Consequently, these results suggested that when the thickness is above several R_g the mobility of polymer chains increases with the decrease of thickness in the presence of CO_2, resulting in the enhanced crystallization kinetics, and when the thickness is about R_g the morphology is governed by the dewetting process.

Enhancing Segmental Mobility of PC in Thin Films by $ScCO_2$. With the above results, we are now in a step to summarize the $ScCO_2$-induced crystallization behavior of PC in thin and ultrathin films, which is distinct from that in the bulk. It is commonly accepted that the plot of the overall crystallization rate as a function of temperature is a bell-shaped curve in the range between T_g and T_m with a maximum value. On the basis of experimental results, three representative schematic curves for PC crystallization in different situations are shown in Figure 7. For the bulk PC at ambient pressure, the overall crystallization rate is extremely slow as mentioned above (curve a). In the presence of $ScCO_2$, the plasticization effect exerted by CO_2 enhances the mobility of polymer chains and depresses T_g, T_m and T_{max}.[40] Accordingly, the crystallization rate curve shifts to lower temperature with an increased maximum crystallization rate (curve b). In the case of thin film/CO_2 system, PC crystallizes in a broader range of temperature and pressure, especially the low limit of temperature for crystallization is greatly reduced (curve c). It might be attributed to the much more decreased T_g of PC in thin film plasticized by CO_2. Therefore, it is suggested

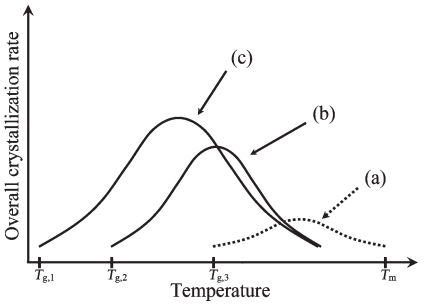

Figure 7. Illustration of curves showing the overall crystallization rate as a function of temperature for three different PC systems. (a) Bulk PC at ambient pressure. (b) Bulk PC in the presence of $ScCO_2$. (c) PC thin and ultrathin films in the presence of $ScCO_2$.

that thin PC films with the thickness ranging from several hundreds of nanometers to about $2R_g$ show crystallization behavior deviating from the polymer bulk, and a reduction in the thickness results in enhanced crystallization kinetics and a widened crystallization temperature range. However, in films with the thickness near the R_g, the crystallization of PC is inhibited. The occurrence of dewetting means that the actual T_g is far below the bulk T_g in CO_2.

The dynamic heterogeneity of a thin film is a complicated issue, and the distribution of the chain mobility and T_g of polymer across film has been focused by considerable efforts.[4−7,9,10,17−19] For a substrate-supported film, the influence of free surface and substrate interface may propagate tens of nanometers into the film interior.[5,9,10,19] Nevertheless, the simple three-layer model proposed by DeMaggio et al[17] is adopted to interpret the results in the present study. It was postulated that the films consist of layers with different mobility and T_g. In the model, a free-surface layer is highly mobile exhibiting reduced T_g relative to bulk T_g,[4,7−10,19] and a substrate-interface layer has strong entropic constraint exerted by the substrate and elevated T_g,[5,16,55,56] and a bulk-like layer exists between these two interfaces, as illustrated in Figure 8a. It should be noticed this model was proposed based on the phenomena observed at atmospheric pressure.

However, the swelling of the polymer thin film by CO_2 would change these three layers in different manners. It is suggested that the excess CO_2 is adsorbed at the thin film surface and substrate interface,[29−32,57] which is entropically favorable by contrast to macromolecules in the bulk, and accordingly the CO_2 sorption and swelling of the thin film in the rubbery state exceed significantly those of the bulk. On the other hand, CO_2 itself can interact with the hydroxyl groups on the substrate,[58] screening the polymer−substrate interaction to decrease the confinement effect in the substrate−interface layer, resulting in enhanced

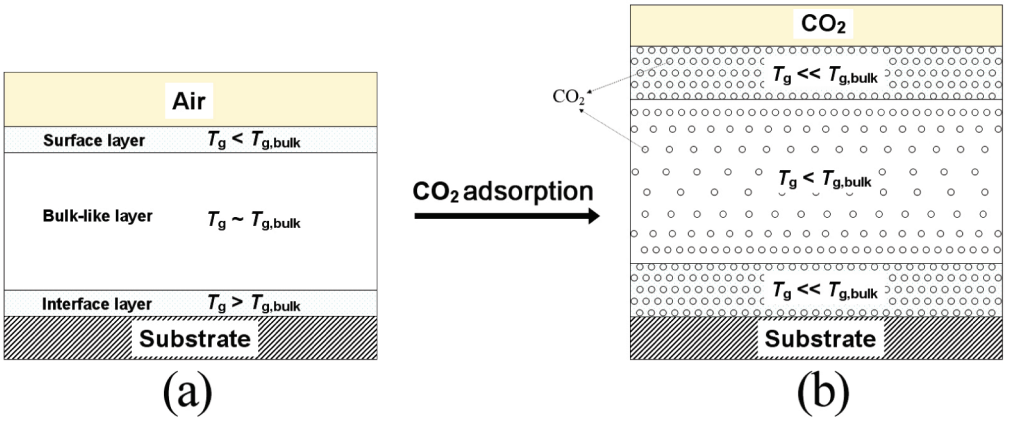

Figure 8. Schematic representation of three-layer mobility model of polymer thin films under ambient pressure (a) and the corresponding CO_2 adsorbed model of polymer films (b).

mobility of polymer chains in the layer.[29,31,32] Therefore, the portions of top and bottom layers in the whole film are increased in the presence of CO_2,[59] both of which contribute positively to the molecular mobility in overall film by comparison with the bulk-like layer (Figure 8b).

In general, at ambient pressure, the thermal and crystallization properties of polymer thin films with thickness above about 100 nm are similar to those of bulk polymer, such as T_g[6,7] and T_m.[49] However, the reduction in crystallinity degree and crystallization rate compared to the bulk polymer usually occur when the thickness decreases to about 50 nm, resulting from the constrained geometry.[3,23,24] In contrast, in the presence of CO_2 the thin PC film exhibits faster crystallization kinetics than the bulk sample because of the existence of two non-negligible layers (surface and interface layers) having high mobility. Moreover, the influence of surface/interface layers on the crystallization behavior would be in working even up to a larger thickness, i.e., 259 nm in this study, and would be enhanced with the decrease of film thickness and increase of treatment pressure. Similarly, it has been reported that the enhanced mobility at the free surfaces can also accelerate physical aging of free-standing glassy polymer thin films up to several hundreds of nanometers thick,[60−62] in comparison to corresponding thicker film or bulk. Also, as a result of an enhanced surface segmental mobility, a faster crystallization kinetics occurs in the region near the free surface of poly(ethylene terephthalate) films.[11] On the other hand, in the case of ultrathin films, the heterogeneous nucleation initiated by the surface/interface plays an important role in the crystallization, preferred to form flat-on lamellae at high temperatures. Therefore, the overall crystallization behavior of PC in thin films is thus different from that in bulk samples, when the portion of high mobility layers with the corresponding plasticization effect increases to a certain degree.

In the present study, the PC thin films are supported on weakly attractive substrate by annealing at a temperature just below the bulk T_g of PC. It is worth to note that a dead layer, which exhibits no T_g or expansion coefficient, can form in polymer thin film on weakly attractive substrate by annealing at high temperature (normally higher than bulk T_g + 20 K)[63−67] as well as in film when polymer−substrate interaction is strong.[22,67,68] Such a layer is stable against washing by a good solvent of the polymer. Therefore, further effort is required to investigate whether the annealing conditions (temperature and time) influence the crystallization behavior of thin polymer films in the presence of CO_2.

CONCLUSIONS

Thin PC films with the thickness between 10^2-10^0 nanometers were treated in $ScCO_2$ over a wide pressure and temperature range. The influence of treatment conditions on the crystallization behavior of thin PC films was investigated on the basis of observed POM and AFM morphologies. The thin film of 259 nm was induced to crystallize in a wider temperature range in the presence of CO_2 by comparison with bulk sample, and the crystallization window was further broadened when the thickness of samples decreased. It indicates that polymer chain mobility is increased with the decrease of thickness in these thin film/CO_2 samples.

The effect of CO_2 adsorption was introduced to the three-layer model to interpret the enhanced polymer chain mobility and the resultant crystallization rate of thin PC films in $ScCO_2$. CO_2 was adsorbed excessively in both free surface and substrate-interface layers, and screened interaction between substrate and polymer in thin films. Consequently, the proportion having high molecular mobility was increased to enhance overall mobility of film throughout the thickness range studied. Moreover, the effect of surface/interface layers on the crystallization behavior became significantly with the decrease of the film thickness. Under CO_2 at a lower pressure of 8 MPa, the film with thinner thickness (45 nm) crystallized completely at a low temperature of 160 °C, while the thicker one (259 nm) merely formed incomplete crystals irrespective of the treatment temperature. The film of 15 nm thick crystallized at low temperatures far below the bulk T_g, while the 259 nm thick film remained amorphous. Meanwhile, dewetting process took place for the film of 7 nm thick, instead of crystallization. On the other hand, CO_2 adsorption increased with the increase of pressure to amplify the effect of surface/interface layers in thin PC films, resulting in enhanced maximum rate for crystallization and shift of T_{max} to lower temperature. These results of thin PC films under $ScCO_2$ are of significant importance to get more direct insight into the specific crystallization behavior of thin polymer films.

AUTHOR INFORMATION

Corresponding Author

*Fax +86 10 6261 3251. E-mail: (J.Y.) yuj@iccas.ac.cn; (J.Z.) jzhang@iccas.ac.cn.

■ ACKNOWLEDGMENT

We thank National Natural Science Foundation of China (Grant No. 20774106, No. 50821602), National Basic Research Program of China (973 Program, No. 2010CB934705), Knowledge Innovation Program of the Chinese Academy of Sciences (No. KJCX2.YW.H16, No. KJCX2.YW.H19), and National Key Technology R & D Program (No. 2009AA033601) for financial support.

■ REFERENCES

(1) Wu, W. L.; Vanzanten, J. H.; Orts, W. J. *Macromolecules* **1995**, *28*, 771–774.
(2) Atashbar, M. Z.; Bejcek, B.; Vijh, A.; Singamaneni, S. *Sens. Actuator B: Chem.* **2005**, *107*, 945–951.
(3) Frank, C. W.; Rao, V.; Despotopoulou, M. M.; Pease, R. F. W.; Hinsberg, W. D.; Miller, R. D.; Rabolt, J. F. *Science* **1996**, *273*, 912–915.
(4) Keddie, J. L.; Jones, R. A. L.; Cory, R. A. *Europhys. Lett.* **1994**, *27*, 59–64.
(5) Keddie, J. L.; Jones, R. A. L.; Cory, R. A. *Faraday Discuss.* **1994**, *98*, 219–230.
(6) Forrest, J. A.; Dalnoki-Veress, K. *Adv. Colloid Interface Sci.* **2001**, *94*, 167–196.
(7) Forrest, J. A.; Dalnoki-Veress, K.; Stevens, J. R.; Dutcher, J. R. *Phys. Rev. Lett.* **1996**, *77*, 2002–2005.
(8) Kerle, T.; Lin, Z. Q.; Kim, H. C.; Russell, T. P. *Macromolecules* **2001**, *34*, 3484–3492.
(9) Kawaguchi, D.; Tanaka, K.; Kajiyama, T.; Takahara, A.; Tasaki, S. *Macromolecules* **2003**, *36*, 1235–1240.
(10) Jones, R. A. L. *Nat. Mater.* **2003**, *2*, 645–646.
(11) Jukes, P. C.; Das, A.; Durell, M.; Trolley, D.; Higgins, A. M.; Geoghegan, M.; Macdonald, J. E.; Jones, R. A. L.; Brown, S.; Thompson, P. *Macromolecules* **2005**, *38*, 2315–2320.
(12) Roth, C. B.; Dutcher, J. R. *Eur. Phys. J. E* **2003**, *12*, S103–S107.
(13) van Zanten, J. H.; Wallace, W. E.; Wu, W. L. *Phys. Rev. E* **1996**, *53*, R2053–R2056.
(14) Prucker, O.; Christian, S.; Bock, H.; Ruhe, J.; Frank, C. W.; Knoll, W. *Macromol. Chem. Phys.* **1998**, *199*, 1435–1444.
(15) Fryer, D. S.; Nealey, P. F.; de Pablo, J. J. *Macromolecules* **2000**, *33*, 6439–6447.
(16) Grohens, Y.; Hamon, L.; Reiter, G.; Soldera, A.; Holl, Y. *Eur. Phys. J. E* **2002**, *8*, 217–224.
(17) DeMaggio, G. B.; Frieze, W. E.; Gidley, D. W.; Zhu, M.; Hristov, H. A.; Yee, A. F. *Phys. Rev. Lett.* **1997**, *78*, 1524–1527.
(18) Fryer, D. S.; Peters, R. D.; Kim, E. J.; Tomaszewski, J. E.; de Pablo, J. J.; Nealey, P. F.; White, C. C.; Wu, W. L. *Macromolecules* **2001**, *34*, 5627–5634.
(19) Ellison, C. J.; Torkelson, J. M. *Nat. Mater.* **2003**, *2*, 695–700.
(20) Ellison, C. J.; Mundra, M. K.; Torkelson, J. M. *Macromolecules* **2005**, *38*, 1767–1778.
(21) Ellison, C. J.; Ruszkowski, R. L.; Fredin, N. J.; Torkelson, J. M. *Phys. Rev. Lett.* **2004**, *92*, 095702.
(22) Tsui, O. K. C.; Russell, T. P.; Hawker, C. J. *Macromolecules* **2001**, *34*, 5535–5539.
(23) Mareau, V. H.; Prud'homme, R. E. *Macromolecules* **2005**, *38*, 398–408.
(24) Despotopoulou, M. M.; Miller, R. D.; Rabolt, J. F.; Frank, C. W. *J. Polym. Sci., Part B: Polym. Phys.* **1996**, *34*, 2335–2349.
(25) Reiter, G.; Sommer, J. U. *Phys. Rev. Lett.* **1998**, *80*, 3771–3774.
(26) Reiter, G.; Sommer, J. U. *J. Chem. Phys.* **2000**, *112*, 4376–4383.
(27) Wang, Y.; Chan, C. M.; Ng, K. M.; Li, L. *Macromolecules* **2008**, *41*, 2548–2553.
(28) Koga, T.; Seo, Y. S.; Hu, X.; Shin, K.; Zhang, Y.; Rafailovich, M. H.; Sokolov, J. C.; Chu, B.; Satija, S. K. *Europhys. Lett.* **2002**, *60*, 559–565.
(29) Sirard, S. M.; Ziegler, K. J.; Sanchez, I. C.; Green, P. F.; Johnston, K. P. *Macromolecules* **2002**, *35*, 1928–1935.
(30) Li, Y.; Park, E. J.; Lim, K. T. L.; Johnston, K. P.; Green, P. F. *J. Polym. Sci., Part B: Polym. Phys.* **2007**, *45*, 1313–1324.
(31) Pham, J. Q.; Johnston, K. P.; Green, P. F. *J. Phys. Chem. B* **2004**, *108*, 3457–3461.
(32) Pham, J. Q.; Sirard, S. M.; Johnston, K. P.; Green, P. F. *Phys. Rev. Lett.* **2003**, *91*, 175503.
(33) Tomasko, D. L.; Li, H. B.; Liu, D. H.; Han, X. M.; Wingert, M. J.; Lee, L. J.; Koelling, K. W. *Ind. Eng. Chem. Res.* **2003**, *42*, 6431–6456.
(34) Ma, W. M.; Yu, J.; He, J. S. *Macromolecules* **2005**, *38*, 4755–4760.
(35) Ma, W. M.; Yu, J.; He, J. S. *Macromol. Rapid Commun.* **2005**, *26*, 112–115.
(36) Gross, S. M.; Roberts, G. W.; Kiserow, D. J.; DeSimone, J. M. *Macromolecules* **2000**, *33*, 40–45.
(37) Beckman, E.; Porter, R. S. *J. Polym. Sci., Part B: Polym. Phys.* **1987**, *25*, 1511–1517.
(38) Condo, P. D.; Sanchez, I. C.; Panayiotou, C. G.; Johnston, K. P. *Macromolecules* **1992**, *25*, 6119–6127.
(39) Zhang, Z. Y.; Handa, Y. P. *Macromolecules* **1997**, *30*, 8505–8507.
(40) Zhai, W. T.; Yu, J.; Ma, W. M.; He, J. S. *Macromolecules* **2007**, *40*, 73–80.
(41) Gallez, F.; Legras, R.; Mercier, J. P. *J. Polym. Sci., Part B: Polym. Phys.* **1976**, *14*, 1367–1377.
(42) Gallez, F.; Legras, R.; Mercier, J. P. *Polym. Eng. Sci.* **1976**, *16*, 276–283.
(43) Turska, E.; Janeczek, H. *Polymer* **1979**, *20*, 855–858.
(44) Legras, R.; Mercier, J. P.; Nield, E. *Nature* **1983**, *304*, 432–434.
(45) Siegmann, A.; Geil, P. H. *J. Macromol. Sci.—Phys.* **1970**, *B4*, 239–271.
(46) Andersson, A.; Zhai, W. T.; Yu, J.; He, J. S.; Maurer, F. H. J. *Polymer* **2010**, *51*, 146–152.
(47) Lan, Q. F.; Yu, J.; He, J. S.; Maurer, F. H. J.; Zhang, J. *Macromolecules* **2010**, *43*, 8602–8609.
(48) Zhang, Z. Y.; Handa, Y. P. *J. Polym. Sci., Part B: Polym. Phys.* **1998**, *36*, 977–982.
(49) Wang, Y.; Ge, S.; Rafailovich, M.; Sokolov, J.; Zou, Y.; Ade, H.; Luning, J.; Lustiger, A.; Maron, G. *Macromolecules* **2004**, *37*, 3319–3327.
(50) Brener, E.; Muller-Krumbhaar, H.; Temkin, D. *Phys. Rev. E* **1996**, *54*, 2714–2722.
(51) Qiao, C. D.; Zhao, J. C.; Jiang, S. C.; Ji, X. L.; An, L. J.; Jiang, B. Z. *J. Polym. Sci., Part B: Polym. Phys.* **2005**, *43*, 1303–1309.
(52) Tang, M.; Du, T. B.; Chen, Y. P. *J. Supercrit. Fluids* **2004**, *28*, 207–218.
(53) Reiter, G. *Phys. Rev. Lett.* **1992**, *68*, 75–78.
(54) Reiter, G. *Macromolecules* **1994**, *27*, 3046–3052.
(55) Bitsanis, I.; Hadziioannou, G. *J. Chem. Phys.* **1990**, *92*, 3827–3847.
(56) Baschnagel, J.; Binder, K. *Macromolecules* **1995**, *28*, 6808–6818.
(57) Sirard, S. M.; Green, P. F.; Johnston, K. P. *J. Phys. Chem. B* **2001**, *105*, 766–772.
(58) Strubinger, J. R.; Parcher, J. F. *Anal. Chem.* **1989**, *61*, 951–955.
(59) Yang, Y.; Cheng, M. M. C.; Hu, X.; Liu, D. H.; Goyette, R. J.; Lee, L. J.; Ferrari, M. *Macromolecules* **2007**, *40*, 1108–1111.
(60) McCaig, M. S.; Paul, D. R. *Polymer* **2000**, *41*, 629–637.
(61) Huang, Y.; Paul, D. R. *Macromolecules* **2006**, *39*, 1554–1559.
(62) Rowe, B. W.; Pas, S. J.; Hill, A. J.; Suzuki, R.; Freeman, B. D.; Paul, D. R. *Polymer* **2009**, *50*, 6149–6156.
(63) Soles, C. L.; Douglas, J. F.; Wu, W. L.; Peng, H. G.; Gidley, D. W. *Macromolecules* **2004**, *37*, 2890–2900.
(64) Napolitano, S.; Wubbenhorst, M. *J. Phys. Chem. B* **2007**, *111*, 9197–9199.
(65) Rotella, C.; Napolitano, S.; De Cremer, L.; Koeckelberghs, G.; Wubbenhorst, M. *Macromolecules* **2010**, *43*, 8686–8691.
(66) Napolitano, S.; Pilleri, A.; Rolla, P.; Wubbenhorst, M. *ACS Nano* **2010**, *4*, 841–848.
(67) Fujii, Y.; Yang, Z. H.; Leach, J.; Atarashi, H.; Tanaka, K.; Tsui, O. K. C. *Macromolecules* **2009**, *42*, 7418–7422.
(68) Xue, L. J.; Han, Y. C. *Langmuir* **2009**, *25*, 5135–5140.